

# A Bramble-Pasciak Conjugate Gradient Method for Discrete Stokes Problems with Lognormal Random Viscosity

Christopher Müller<sup>1,2</sup>, Sebastian Ullmann<sup>1,2</sup>, and Jens Lang<sup>1,2</sup>

<sup>1</sup> Graduate School of Computational Engineering, Technische Universität Darmstadt, Dolivostr. 15, 64293, Darmstadt, Germany

cmueller@gsc.tu-darmstadt.de,

WWW home page: <http://www.graduate-school-ce.de/index.php?id=680>

<sup>2</sup> Department of Mathematics, Technische Universität Darmstadt, Dolivostr. 15, 64293, Darmstadt, Germany

**Abstract.** We study linear systems of equations arising from a stochastic Galerkin finite element discretization of saddle point problems with random data and its iterative solution. We consider the Stokes flow model with random viscosity described by the exponential of a correlated random process and shortly discuss the discretization framework and the representation of the emerging matrix equation. Due to the high dimensionality and the coupling of the associated symmetric, indefinite, linear system, we resort to iterative solvers and problem-specific preconditioners. As a standard iterative solver for this problem class, we consider the block diagonal preconditioned MINRES method and further introduce the Bramble-Pasciak conjugate gradient method as a promising alternative. This special conjugate gradient method is formulated in a non-standard inner product with a block triangular preconditioner. From a structural point of view, such a block triangular preconditioner enables a better approximation of the original problem than the block diagonal one. We derive eigenvalue estimates to assess the convergence behavior of the two solvers with respect to relevant physical and numerical parameters and verify our findings by the help of a numerical test case. We model Stokes flow in a cavity driven by a moving lid and describe the viscosity by the exponential of a truncated Karhunen-Loève expansion. Regarding iteration counts, the Bramble-Pasciak conjugate gradient method with block triangular preconditioner is superior to the MINRES method with block diagonal preconditioner in the considered example.

**Keywords:** Uncertainty quantification, PDEs with random data, Stokes flow, Preconditioning, Stochastic Galerkin, Lognormal data, Mixed finite elements, Conjugate gradient method, Saddle point problems

## 1 Introduction

We study the stochastic Galerkin finite element (SGFE) method [2,13,14] as a tool to approximate statistical quantities in the context of saddle point problems

with random input data. Stochastic Galerkin (SG) methods rely on a representation of the random input based on a vector of random variables with known probability density. The starting point of the method is a weak formulation not only over the spatial domain but also over the image domain of this random vector. The SGFE approach enables the computation of the unknown solution coefficients via a Galerkin projection onto the finite dimensional tensor product space of a finite element (FE) space for the spatial dependencies and a global polynomial/SG space for the random vector.

Concerning convergence rates, SG methods are often superior to more robust stochastic methods – such as Monte-Carlo sampling – when the input data exhibits certain regularity structures [4,16]. This is a property shared by the main competitors of the SG approaches: Stochastic collocation methods [3,14] similarly exploit the structure of the random input and further rely on uncoupled solutions of the underlying deterministic problem, just like sampling methods. An advantage of SG methods is that rigorous error analysis can be used to analyze them, but they are more challenging from a computational point of view: A block structured system of coupled deterministic problems must be solved. However, this can be done efficiently using iterative methods and problem-specific preconditioners, see e.g. [11,19,22,24,29].

We build on these results and consider the Bramble-Pasciak conjugate gradient (BPCG) method [7] in the SGFE setting with lognormal data. We compare it to the MINRES approach, the standard Krylov subspace solver for the problem class we consider, and investigate the performance of both solvers with respect to different problem and discretization parameters. This is done both analytically and based on a numerical test case.

As a saddle point problem, we consider the Stokes flow model in a bounded domain  $D \subset \mathbb{R}^2$  with boundary  $\partial D$ . The vector  $x = (x_1, x_2)^T \in D$  denotes the spatial coordinates. The Stokes equations are a simplification of the Navier-Stokes equations and describe the behavior of a velocity field  $u = (u_1, u_2)^T$  and a pressure field  $p$  subject to viscous and external forcing. We also introduce the probability space  $(\Omega, \mathcal{F}, \mathbb{P})$ , where  $\Omega$  denotes the set of elementary events,  $\mathcal{F}$  is a  $\sigma$ -algebra on  $\Omega$  and  $\mathbb{P} : \mathcal{F} \rightarrow [0, 1]$  is a probability measure.

Input data are inherently uncertain due to either a lack of knowledge or simply imprecise measurements. Taking into account this variability in the model, we assume that the viscosity is a random field  $\nu = \nu(x, \omega) : D \times \Omega \rightarrow \mathbb{R}$ . Since the input uncertainty propagates through the model, the solution components also have to be considered as random fields. In summary, the strong form of the Stokes equations with uncertain viscosity is the following:

Find  $u = u(x, \omega)$  and  $p = p(x, \omega)$  such that,  $\mathbb{P}$ -almost surely,

$$\begin{aligned} -\nabla \cdot (\nu(x, \omega) \nabla u(x, \omega)) + \nabla p(x, \omega) &= f(x) && \text{in } D \times \Omega, \\ \nabla \cdot u(x, \omega) &= 0 && \text{in } D \times \Omega, \\ u(x, \omega) &= g(x) && \text{on } \partial D \times \Omega. \end{aligned} \tag{1}$$

Both, the volume force  $f = (f_1, f_2)^T$  and the boundary data  $g = (g_1, g_2)^T$  are assumed to be deterministic functions. This is for the sake of simplicity of

notation. Treating stochastic forcing and boundary data in the model would be straightforward under appropriate integrability assumptions on the data.

The remainder of the paper is organized as follows: As a model for the uncertain viscosity, we introduce the exponential of a Karhunen-Loève expansion (KLE) of a Gaussian random field in section 2. We ensure boundedness of this expansion by stating suitable assumptions on its components. The boundedness of the viscosity is necessary for the well-posedness of the variational formulation we introduce in section 3. In section 4, we establish a matrix representation of the Stokes problem with lognormal random data by restricting the weak equations to a finite dimensional subspace spanned by Taylor-Hood finite elements and Hermite chaos polynomials. Preconditioning strategies are discussed in section 5 where we consider block diagonal and block triangular preconditioning structures. As building blocks, we use a Kronecker product structure with established approaches from the FE and SG literature as input. In section 6, we derive inclusion bounds for the eigenvalues of relevant sub-matrices and interpret them concerning the overall convergence behavior. By modifying our block triangular preconditioner in a specific way, we ensure the existence of a conjugate gradient (CG) method in a non-standard inner product. We discuss the application of this CG method as well as the application of the MINRES iterative solver in greater detail in section 7. A numerical test case is considered in section 8 where we illustrate the expected convergence behavior of the two considered solvers with respect to different problem parameters. The final section eventually summarizes and concludes our work.

## 2 Input Modeling

We start our considerations with the random field  $\mu(x, \omega)$  and assume that it is Gaussian and second-order, meaning  $\mu \in L^2(\Omega, L^2(D))$ . In this setting it is possible to represent  $\mu(x, \omega)$  as a KLE of the form [18, Theorem 5.28]

$$\mu(x, \omega) = \mu_0(x) + \sigma_\mu \sum_{m=1}^{\infty} \sqrt{\lambda_m} \mu_m(x) y_m(\omega). \quad (2)$$

Here,  $\mu_0(x)$  is the mean field of  $\mu(x, \omega)$ , i.e.  $\mu_0(x) = \int_{\Omega} \mu(x, \omega) d\mathbb{P}(\omega)$  is the expected value of the random field. The eigenpairs  $(\lambda_m, \mu_m)_{m=1}^{\infty}$  belong to the integral operator which corresponds to the covariance function of the correlated Gaussian random field. Further,  $y_m, m = 1, \dots, \infty$ , are uncorrelated Gaussian random variables with zero mean and unit variance which live in the unbounded set of sequences  $\mathbb{R}^{\mathbb{N}}$ . As we are in the Gaussian setting, the random variables originating from the KLE are also stochastically independent.

The unbounded support of the Gaussian random variables leads to one major problem concerning the theoretical investigations of the problem: As there is always a nonzero probability that random variables take on negative values with arbitrarily large magnitudes, negative values of the modeled viscosity can occur independent of its construction. We use a standard approach to avoid negative

values and apply the exponential function to (2), yielding

$$\nu(x, \omega) = \exp(\mu(x, \omega)) = \exp\left(\mu_0(x) + \sigma_\mu \sum_{m=1}^{\infty} \sqrt{\lambda_m} \mu_m(x) y_m(\omega)\right), \quad (3)$$

for  $y = (y_m(\omega))_{m \in \mathbb{N}} : \Omega \rightarrow \mathbb{R}^{\mathbb{N}}$ . Expression (3) is called a lognormal random process as the logarithm of  $\nu(x, \omega)$  is the Gaussian process  $\mu(x, \omega)$ . In order to ensure boundedness of the viscosity, some assumptions have to be made on the series components. Following [16], we assume that

(i) the mean field of  $\mu(x, \omega)$  and the product of the Karhunen-Loève eigenpairs is bounded:

$$\mu_0, \sqrt{\lambda_m} \mu_m \in L^\infty(D), \quad \forall m \in \mathbb{N}, \quad (4)$$

(ii) the series of the product of the Karhunen-Loève eigenpairs converges absolutely:

$$\chi := (\chi_m)_{m \geq 1} = (\|\sqrt{\lambda_m} \mu_m(x)\|_{L^\infty(D)})_{m \geq 1} \in \ell^1(\mathbb{N}). \quad (5)$$

Then, we define the set

$$\Xi^M := \mathbb{R}^M.$$

The set  $\Xi^M$  can also be defined for infinitely many parameters. However, we will not do this here as it introduces additional difficulties to the problem. For a full analysis, we refer to [25].

We define the value  $\bar{\mu}_0 := \|\mu_0(x)\|_{L^\infty(D)}$  and the truncated viscosity:

$$\nu_M(x, y) = \exp\left(\mu_0(x) + \sigma_\mu \sum_{m=1}^M \sqrt{\lambda_m} \mu_m(x) y_m\right), \quad (6)$$

for  $y \in \Xi^M$ . Given the assumptions (4) and (5), the viscosity (6) satisfies

$$0 < \underline{\nu}(y) := \operatorname{ess\,inf}_{x \in D} \nu_M(x, y) \leq \nu_M(x, y) \leq \operatorname{ess\,sup}_{x \in D} \nu_M(x, y) =: \bar{\nu}(y), \quad (7)$$

with

$$\begin{aligned} \bar{\nu}(y) &\leq \exp(\bar{\mu}_0) \exp\left(\sum_{m=1}^M \chi_m |y_m|\right), \\ \underline{\nu}(y) &\geq \exp(-\bar{\mu}_0) \exp\left(-\sum_{m=1}^M \chi_m |y_m|\right), \end{aligned}$$

for  $y \in \Xi^M$ . A proof of (7) can be found in [16, Lemma 2.2].

As a consequence of (7), the viscosity (3) is bounded from above and has a positive lower bound for almost all  $\omega \in \Omega$ . This is a basic property necessary for our problem to be well-defined. A reasonable truncation is possible with moderate  $M$  when the covariance operator of the underlying random field is sufficiently smooth and the correlation length is sufficiently large.

The stochastic independence of the random variables allows us to express the corresponding Gaussian density as a product of univariate densities:

$$\rho(y) := \prod_{m=1}^M \rho_m(y_m), \quad \text{with} \quad \rho_m(y_m) := \frac{1}{\sqrt{2\pi}} \exp(-y_m^2/2). \quad (8)$$

It makes sense to change from the abstract the domain  $\Xi^M$  in the following, see [16, section 2.1]. The change of the space leads to an integral transform, such that the computation of the  $p$ th moment of a random variable  $v(\omega)$  is done via

$$\int_{\Omega} v^p(\omega) \, d\mathbb{P}(\omega) \approx \int_{\Xi^M} v^p(y) \rho(y) \, dy =: \langle v^p \rangle. \quad (9)$$

As a consequence of the Doob-Dynkin lemma [20], the output random fields can be parametrized with the vector  $y$  as well.

### 3 Variational Formulation

In order to formulate the weak equations derived from (1), we introduce Bochner spaces  $L_{\rho}^2(\Xi^M; X)$ , where  $X$  is a separable Hilbert space. They consist of all equivalence classes of strongly measurable functions  $v : \Xi^M \rightarrow X$  with norm

$$\|v\|_{L_{\rho}^2(\Xi^M; X)} = \left( \int_{\Xi^M} \|v(\cdot, y)\|_X^2 \rho(y) \, dy \right)^{1/2} < \infty.$$

In the following, we work in the tensor product spaces  $L_{\rho}^2(\Xi^M) \otimes X$  with corresponding norms  $\|\cdot\|_{L_{\rho}^2(\Xi^M) \otimes X} := \|\cdot\|_{L_{\rho}^2(\Xi^M; X)}$  as they are isomorphic to the Bochner spaces for separable  $X$ .

For the Stokes problem with random data, we insert the standard function spaces for enclosed flow and introduce

$$\begin{aligned} \mathbf{V}_0 &:= L_{\rho}^2(\Xi^M) \otimes \mathbf{V}_0(D), \\ \mathcal{W}_0 &:= L_{\rho}^2(\Xi^M) \otimes W_0(D), \end{aligned} \quad (10)$$

with

$$\begin{aligned} \mathbf{V}_0 &:= \mathbf{H}_0^1(D) = \left\{ v \in \mathbf{H}^1(D) \mid v|_{\partial D} = 0 \right\}, \\ \mathcal{W}_0 &:= L_0^2(D) = \left\{ q \in L^2(D) \mid \int_D q(x) \, dx = 0 \right\}. \end{aligned}$$

The product spaces are Hilbert spaces as well.

We are now able to formulate the variational formulation associated with (1): Find  $(u, p) \in \mathbf{V}_0 \times \mathcal{W}_0$  satisfying

$$\begin{aligned} \langle a(u, v) \rangle + \langle b(v, p) \rangle &= \langle l(v) \rangle, & \forall v \in \mathbf{V}_0, \\ \langle b(u, q) \rangle &= \langle t(q) \rangle, & \forall q \in \mathcal{W}_0, \end{aligned} \quad (11)$$

with bilinear forms

$$\langle a(u, v) \rangle := \int_{\Xi^M} \int_D \nu_M(x, y) \nabla u(x, y) \cdot \nabla v(x, y) \rho(y) \, dx \, dy, \quad (12)$$

$$\langle b(v, q) \rangle := - \int_{\Xi^M} \int_D q(x, y) \nabla \cdot v(x, y) \rho(y) \, dx \, dy, \quad (13)$$

for  $u, v \in \mathcal{V}_0$ ,  $q \in \mathcal{W}_0$ , and linear functionals

$$\langle l(v) \rangle := \int_{\Xi^M} \int_D f(x) \cdot v(x, y) \rho(y) \, dx \, dy - \langle a(u_0, v) \rangle, \quad \forall v \in \mathcal{V}_0,$$

$$\langle t(v) \rangle := -\langle b(u_0, q) \rangle, \quad \forall q \in \mathcal{W}_0,$$

where  $u_0 \in \mathcal{V}_0$  is the lifting of the boundary data  $g$  in the sense of the trace theorem.

The weak equations (11) are a set of parametric deterministic equations which contain the full stochastic information of the original problem with random data. For the well-posedness of the variational formulation (11), we refer to [25].

## 4 Stochastic Galerkin Finite Element Discretization

We derive a discrete set of equations from (11) by choosing appropriate subspaces for the building blocks of the product spaces (10). For the discretization of the physical space, we use FE subspaces  $\mathbf{V}_0^h \subset \mathbf{V}_0$  and  $W_0^h \subset W_0$ , where  $h$  denotes the mesh size. The domain of the random variables is discretized with generalized polynomial chaos [31]. The corresponding SG space is denoted by  $S^k \subset L_\rho^2(\Xi^M)$ , where  $k$  is the degree of the chaos functions and  $M$  is the truncation index of the KLE in (6). The SGFE subspaces  $\mathcal{V}_0^{kh} \subset \mathcal{V}_0$  and  $\mathcal{W}_0^{kh} \subset \mathcal{W}_0$  are now defined as products of the separate parts:

$$\begin{aligned} \mathcal{V}_0^{kh} &:= S^k \otimes \mathbf{V}_0^h, \\ \mathcal{W}_0^{kh} &:= S^k \otimes W_0^h. \end{aligned} \quad (14)$$

As a specific choice for the spatial discretization, we use inf-sup stable Taylor-Hood  $P_2/P_1$  finite elements on a regular triangulation. They consist of  $N_u$  continuous piecewise quadratic basis functions for the velocity space and  $N_p$  continuous piecewise linear basis functions for the pressure space. For the parametric space, we choose a discretization based on a complete multivariate Hermite polynomial chaos. The corresponding basis functions are global polynomials which are orthonormal with respect to the joint density  $\rho(y)$  in (8). Therefore, they are the appropriate match to the Gaussian distribution of the input parameters according to the Wiener-Askey scheme [31]. We construct the  $M$ -variate basis functions as a product of  $M$  univariate chaos polynomials. We work with a complete polynomial basis, i.e. we choose a total degree  $k$  and the sum of the degrees of the  $M$  univariate chaos polynomials  $\sum_{m=1}^M k_m$  must be less than or equal to  $k$ . This yields a multivariate chaos or stochastic Galerkin basis of size  $Q_z$ , where

$$Q_z := \binom{M+k}{k}. \quad (15)$$

Behind every index  $q = 0, \dots, Q_z - 1$  there is a unique combination of univariate polynomial degrees – a multi-index –  $(k_1, \dots, k_M)$  and vice versa. The  $q$ th multivariate polynomial chaos basis function is thus the product of  $M$  univariate chaos polynomials with degrees from the  $q$ th multi-index.

Regarding the representation (6), a separation of the spatial and parametric dependencies would be beneficial. Such a decomposition can be achieved by representing the exponential of the truncated KLE in a Hermite chaos basis [24]:

$$\nu_M(x, y) = \sum_{q=0}^{Q_\nu-1} \nu_q(x) \psi_q(y), \quad (16)$$

where the  $\{\psi_q(y)\}_{q=0}^{Q_\nu-1}$  are the Hermite chaos basis functions and

$$\nu_q(x) = \exp\left(\mu_0(x) + \frac{1}{2}\sigma_\mu^2 \sum_{m=1}^M \lambda_m \mu_m^2(x)\right) \prod_{m=1}^M \frac{(\sigma_\mu \sqrt{\lambda_m} \mu_m(x))^{k_m}}{\sqrt{k_m!}}. \quad (17)$$

Again, there is a unique multi-index  $(k_1, \dots, k_M)$  to every index  $q = 1, \dots, Q_\nu$ .

When used in a stochastic Galerkin setting, the representation (16) is in fact exact if we use the same Hermite polynomial chaos basis as for the representation of the solution fields but with twice the total degree [26, Remark 2.3.4], i.e.

$$Q_\nu := \binom{M + 2k}{2k}. \quad (18)$$

Although  $Q_\nu$  grows fast with  $k$  and  $M$  and can be a lot bigger than  $Q_z$ , it does not make sense to truncate the sum in (16) prematurely. Doing so may destroy the coercivity of (12) and the corresponding discrete operator can easily become indefinite, see [26, Example 2.3.6]. Consequently, we always use all terms in (16).

Without going into the details, we will assume in the following that the fully discrete problem is well-posed which implies that the discretizations we choose are inf-sup stable on the discrete product spaces (14). An analysis of discrete inf-sup stability for a mixed formulation of the diffusion problem with uniform random data can be found in [6, Lemma 3.1].

The size of the emerging system of equations for our chosen discretizations is

$$\dim(\mathbf{V}_0^{kh} \times \mathcal{W}_0^{kh}) = Q_z (N_u + N_p) = Q_z N. \quad (19)$$

To derive a matrix equation of the Stokes problem with random data, the velocity and pressure random fields as well as the test functions are represented in the FE and SG bases and subsequently inserted into the weak formulation (11) together with the input representation (16), yielding

$$\mathcal{C} \mathbf{w} = \mathbf{b}, \quad \mathcal{C} \in \mathbb{R}^{Q_z N \times Q_z N}, \quad (20)$$

where

$$\mathcal{C} := \begin{bmatrix} \mathcal{A} & \mathcal{B}^T \\ \mathcal{B} & 0 \end{bmatrix}, \quad \mathbf{w} := \begin{bmatrix} \mathbf{u} \\ \mathbf{p} \end{bmatrix}, \quad \mathbf{b} := \begin{bmatrix} \mathbf{f} \\ \mathbf{t} \end{bmatrix}. \quad (21)$$

Here, the vectors  $\mathbf{u} \in \mathbb{R}^{Q_z N_u}$  and  $\mathbf{p} \in \mathbb{R}^{Q_z N_p}$  contain the coefficients of the discrete velocity and pressure solutions, respectively. Furthermore,

$$\mathcal{A} = I \otimes A_0 + \sum_{q=1}^{Q_\nu-1} G_q \otimes A_q \in \mathbb{R}^{Q_z N_u \times Q_z N_u}, \quad (22)$$

$$\mathcal{B} = I \otimes B \in \mathbb{R}^{Q_z N_p \times Q_z N_u}, \quad (23)$$

$$\mathbf{f} = \mathbf{g}_0 \otimes \mathbf{w} \in \mathbb{R}^{Q_z N_u}, \quad (24)$$

$$\mathbf{t} = \mathbf{g}_0 \otimes \mathbf{d} \in \mathbb{R}^{Q_z N_p}, \quad (25)$$

where  $I \in \mathbb{R}^{Q_z \times Q_z}$  is the Gramian of  $S^k$ , because the basis is orthonormal. Further, the  $G_q \in \mathbb{R}^{Q_z \times Q_z}$  emerge from the evaluation of the product of three Hermite chaos basis functions in the expectation (9) with  $p = 1$ . They are called stochastic Galerkin matrices in the following. We call the  $A_q \in \mathbb{R}^{N_u \times N_u}$  weighted FE velocity Laplacians as they are FE velocity Laplacians weighted with the functions  $\nu_q(x)$ ,  $q = 0 \dots, Q_\nu - 1$ . The matrices and vectors in (22)–(25) can all be constructed when the FE and SG basis representations are inserted into the variational formulation (11) together with the input representation (16). To avoid confusion, the matrices on the product spaces are calligraphic capital letters whereas the matrices on either the FE or the SG spaces are standard capital letters.

The size of the SGFE system is the product of the size of the FE basis  $N$  and the size of the SG basis  $Q_z$ . Additionally, the problem is coupled, as the symmetric matrices  $G_q$ ,  $q = 1 \dots, Q_\nu - 1$ , are not diagonal. Therefore, realistic problems are often too big to be treated with direct solution methods, which is why iterative algorithms are used instead. The application of iterative methods naturally raises the question of efficient preconditioning due to the inherent ill-conditioning of the problem. For the mentioned reasons, preconditioning and iterative methods are investigated in the following.

## 5 Preconditioning

The SGFE matrix  $\mathcal{C} \in \mathbb{R}^{Q_z N \times Q_z N}$  in (21) is a symmetric saddle point matrix. Therefore, the following factorizations exist:

$$\begin{bmatrix} \mathcal{A} & \mathcal{B}^T \\ \mathcal{B} & 0 \end{bmatrix} = \begin{bmatrix} I & 0 \\ \mathcal{B}\mathcal{A}^{-1} & I \end{bmatrix} \begin{bmatrix} \mathcal{A} & 0 \\ 0 & \mathcal{S} \end{bmatrix} \begin{bmatrix} I & \mathcal{A}^{-1}\mathcal{B}^T \\ 0 & I \end{bmatrix} = \begin{bmatrix} \mathcal{A} & 0 \\ \mathcal{B} & \mathcal{S} \end{bmatrix} \begin{bmatrix} I & \mathcal{A}^{-1}\mathcal{B}^T \\ 0 & I \end{bmatrix}, \quad (26)$$

where  $\mathcal{S} := -\mathcal{B}\mathcal{A}^{-1}\mathcal{B}^T$  is the SGFE Schur complement. In section 4, we have assumed well-posedness of the discrete variational problem. This implies that the discrete version of the bilinear form (12) is continuous and coercive. Inserting the FE and SG basis, the coercivity condition translates into positive definiteness of the matrix  $\mathcal{A}$ . The congruence transform in (26) then implies that the discrete SGFE problem is indefinite as the Schur complement is negative semi-definite by construction.



Motivated by the factorizations (26), we consider block diagonal and block triangular preconditioning structures in the following. In the context of solving saddle point problems, these are well established concepts [5], which are generically given by

$$\mathcal{P}_1 = \begin{bmatrix} \tilde{\mathcal{A}} & 0 \\ 0 & \tilde{\mathcal{S}} \end{bmatrix}, \quad \mathcal{P}_2 = \begin{bmatrix} \tilde{\mathcal{A}} & 0 \\ \mathcal{B} & \tilde{\mathcal{S}} \end{bmatrix}. \quad (27)$$

Here,  $\tilde{\mathcal{A}}$  and  $\tilde{\mathcal{S}}$  are approximations of  $\mathcal{A}$  and  $\mathcal{S}$ , respectively. Choosing these approximations appropriately is the main task of preconditioning. Desirable properties include a reduction of computational complexity and an improvement of the condition of the involved operators.

In the following, we do not directly look for suitable  $\tilde{\mathcal{A}}$  and  $\tilde{\mathcal{S}}$ , but make another structural assumption prior to that. We want each SGFE preconditioner to be the Kronecker product of one FE and one SG preconditioner, i.e.

$$\tilde{\mathcal{A}} := \tilde{G}_A \otimes \tilde{A}, \quad \tilde{\mathcal{S}} := \tilde{G}_S \otimes \tilde{S}, \quad (28)$$

where  $\tilde{A} \in \mathbb{R}^{N_u \times N_u}$  and  $\tilde{S} \in \mathbb{R}^{N_p \times N_p}$  are approximations of the FE operators and the matrices  $\tilde{G}_A, \tilde{G}_S \in \mathbb{R}^{Q_z \times Q_z}$  are approximations of the SG operators. The structural simplifications (28) have two advantages: Firstly, the Kronecker product is trivially invertible. Secondly, if we look into  $\tilde{\mathcal{A}}^{-1}\mathcal{A}$ , we get

$$\tilde{\mathcal{A}}^{-1}\mathcal{A} = \left( \tilde{G}_A^{-1} + \tilde{A}^{-1}A_0 + \sum_{q=1}^{Q_\nu-1} \tilde{G}_A^{-1}G_q \otimes \tilde{A}^{-1}A_q \right). \quad (29)$$

The SG preconditioner  $\tilde{G}_A$  only acts on the SG matrices  $I$  and  $G_q$  and the FE preconditioner  $\tilde{A}$  acts on the weighted FE Laplacians  $A_q$ ,  $q = 0, \dots, Q_\nu - 1$ . This works in the same way for the preconditioned SGFE Schur complement, as we will see in Lemma 3 on page 15. The separation into FE and SG parts thus allows the use of established preconditioners from the FE and SG literature as building blocks for the SGFE preconditioners. Now, we will choose suitable approximations  $\tilde{A}$  and  $\tilde{S}$  to the FE Laplacian and Schur complement, respectively, and suitable approximations  $\tilde{G}_A$  and  $\tilde{G}_S$  to the SG matrices.

### 5.1 Finite Element Matrices

First of all, we consider a preconditioner for the FE Laplacian and derive bounds for the eigenvalues of the preconditioned weighted FE Laplacians. Then, we decide on a preconditioner for the FE Schur complement.

To precondition FE Laplacians, the multigrid method has emerged as one of the most suitable approaches. The first reason for that is the following: one multigrid V-cycle with appropriate smoothing – denoted by  $\tilde{A}_{\text{mg}}$  in the following – is spectrally equivalent to the FE Laplacian  $A$ , see [8, section 2.5]. In this context, spectral equivalence means that there exist positive constants  $\delta$  and  $\Delta$ ,

independent of  $h$ , such that

$$\delta \leq \frac{\mathbf{v}^T A \mathbf{v}}{\mathbf{v}^T \tilde{A}_{\text{mg}} \mathbf{v}} \leq \Delta, \quad \forall \mathbf{v} \in \mathbb{R}^{N_u} \setminus \{\mathbf{0}\}. \quad (30)$$

As the eigenvalues of  $A$  actually depend on the mesh width  $h$  [8, Theorem 3.21], preconditioning with  $\tilde{A}_{\text{mg}}$  thus eliminates this  $h$ -ill-conditioning of  $A$ . The multigrid method is also attractive from a computational point of view as it can be applied with linear complexity. Concerning (30), when the multigrid operator is applied to the weighted FE Laplacians in (22), we derive

$$-\bar{\nu}_q \Delta \leq \frac{\mathbf{v}^T A_q \mathbf{v}}{\mathbf{v}^T \tilde{A}_{\text{mg}} \mathbf{v}} \leq \bar{\nu}_q \Delta, \quad \forall \mathbf{v} \in \mathbb{R}^{N_u} \setminus \{\mathbf{0}\}, \quad (31)$$

where  $\bar{\nu}_q = \|\nu_q(x)\|_{L^\infty(D)}$ , for  $q = 1, \dots, Q_\nu - 1$ . For  $q = 0$ , the lower bound is different, namely  $\underline{\nu}_0 := \inf_{x \in D} \nu_0(x) > 0$ . This bound is tighter because we know that the function  $\nu_0 = \exp(\mu_0(x) + \frac{1}{2}\sigma_\mu^2 \sum_{m=1}^M \lambda_m \mu_m^2(x))$  from (17) is always positive. The functions are in  $L^\infty(D)$  due to the assumptions (4) and the continuity of the exponential function.

The pressure mass matrix  $M_p$  is a good preconditioner for the negative FE Schur complement  $-S = BA^{-1}B^T$ , because the matrices are spectrally equivalent in the sense that [8, Theorem 3.22]

$$\gamma^2 \leq \frac{\mathbf{q}^T BA^{-1}B^T \mathbf{q}}{\mathbf{q}^T M_p \mathbf{q}} \leq 1, \quad \forall \mathbf{q} \in \mathbb{R}^{N_p} \setminus \{\mathbf{0}, \mathbf{1}\}, \quad (32)$$

where  $B$  is the FE divergence matrix and  $\gamma > 0$  is the inf-sup constant of our mixed FE approximation. Further, the notation  $\setminus \{\mathbf{0}, \mathbf{1}\}$  means we exclude all multiples of the constant function, see [8, Section 3.3]. If necessary, we always exclude the hydrostatic pressure in this way in the following. As  $M_p$  has the usual FE sparsity, using it as a preconditioner is too expensive in practice. Therefore, another approximation is considered, namely its diagonal  $D_p := \text{diag}(M_p)$ . It is spectrally equivalent to  $M_p$ , i.e. there exist  $\theta, \Theta > 0$  such that

$$\theta \leq \frac{\mathbf{q}^T M_p \mathbf{q}}{\mathbf{q}^T D_p \mathbf{q}} \leq \Theta, \quad \forall \mathbf{q} \in \mathbb{R}^{N_p} \setminus \{\mathbf{0}\}. \quad (33)$$

The constants  $\theta$  and  $\Theta$  only depend on the degree and type of finite elements used [30]. We use piecewise linear basis functions on triangles in our work, yielding  $\theta = \frac{1}{2}$  and  $\Theta = 2$ . Consequently,  $D_p$  is spectrally equivalent to the negative FE Schur complement. This directly follows from (32) and (33):

$$\theta \gamma^2 \leq \frac{\mathbf{q}^T BA^{-1}B^T \mathbf{q}}{\mathbf{q}^T D_p \mathbf{q}} \leq \Theta, \quad \forall \mathbf{q} \in \mathbb{R}^{N_p} \setminus \{\mathbf{0}, \mathbf{1}\}. \quad (34)$$

Using  $D_p$  as a preconditioner is also attractive from a complexity point of view as it can be applied with linear costs. The bounds (30), (31) and (34), which are

independent of the mesh size, are the basis for analyzing the  $h$ -independence of the preconditioned SGFE saddle point problem later on in section 6.

Due to the mentioned reasons, we use the multigrid V-cycle and the diagonal of the pressure mass matrix as FE sub-blocks in (28), fixing the choices

$$\tilde{A} := \tilde{A}_{\text{mg}}, \quad \tilde{S} := D_p. \quad (35)$$

## 5.2 Stochastic Galerkin Matrices

The SG preconditioners are also chosen according to complexity considerations and their spectral properties. In particular, we want to improve the condition of the SG matrices with respect to the discretization parameters  $k$  and  $M$  if possible. For the SG matrices based on a product of complete multivariate Hermite polynomials, there exist the following inclusion bounds [24, Corollary 4.5]:

$$-g_q \leq \frac{\mathbf{a}^T G_q \mathbf{a}}{\mathbf{a}^T \mathbf{a}} \leq g_q, \quad \forall \mathbf{a} \in \mathbb{R}^{Q_z} \setminus \{\mathbf{0}\}, \quad (36)$$

for  $q = 1, \dots, Q_\nu - 1$ , where  $g_q = \exp(M(k+1)/2 + \frac{1}{2} \sum_{m=1}^M k_m)$ . As mentioned in section 4 on page 6, the degrees  $k_m$  are the entries of the multi-index associated with the index  $q$ . According to the bounds (36), the eigenvalues of the SG matrices depend on the chaos degree  $k$  and the truncation index  $M$  of the KLE.

In the context of SGFE problems, the mean-based approximation [22] is often used to construct preconditioners for SG matrices. To define an SG preconditioner, the mean information of the SGFE problem is used. We work with an orthonormal chaos basis and the corresponding SG matrix of the mean problem is the identity matrix, see (22). According to our structural ansatz (28), we thus define

$$\tilde{G}_A = \tilde{G}_S = I. \quad (37)$$

We solely use this choice in the following although these preconditioners can not improve the condition of the SG matrices with respect to  $k$  or  $M$ . This is because of two reasons: The mean-based preconditioner is extremely cheap to apply and – to the best of our knowledge – there is no practical preconditioner which can eliminate the ill-conditioning with respect to  $k$ . There is still the potential ill-conditioning with respect to  $M$ . However, our numerical experiments in section 8 suggest that the influence of  $M$  is not that severe.

## 6 Eigenvalue Analysis for the SGFE Matrices

In section 5, we fixed the structures and building blocks of our preconditioners. As a next step, we summarize our assumptions and choices to define the specific preconditioners we eventually use. Starting point for the construction of the preconditioners are the structures (27) and the substructural Kronecker product ansatz (28).

Inserting  $\tilde{A} = \tilde{A}_{\text{mg}}$  and  $\tilde{S} = D_p$  as FE preconditioners, and  $\tilde{G}_A = \tilde{G}_S = I$  as SG preconditioners, we define:

$$\mathcal{P}_{\text{diag}} := \begin{bmatrix} \tilde{A}_{\text{mg}} & 0 \\ 0 & \tilde{S}_p \end{bmatrix}, \quad \mathcal{P}_{\text{tri}} := \begin{bmatrix} a \tilde{A}_{\text{mg}} & 0 \\ \mathcal{B} & -\tilde{S}_p \end{bmatrix}, \quad (38)$$

where

$$\tilde{\mathcal{A}}_{\text{mg}} := I \otimes \tilde{A}_{\text{mg}}, \quad (39)$$

$$\tilde{\mathcal{S}}_p := I \otimes D_p. \quad (40)$$

Both, the negative sign of the Schur complement approximation  $-\tilde{S}_p$  as well as the scalar  $a \in \mathbb{R}$  in the definition of the block triangular preconditioner  $\mathcal{P}_{\text{tri}}$  are manipulations which are not necessary in general. However, they are essential for one of the iterative solvers we are using. The specific effects of these additional manipulations are specified in subsection 6.2.

In order to assess the influence of different problem parameters on the spectrum of the preconditioned SGFE systems, we want to derive inclusion bounds for the eigenvalues of  $\mathcal{P}_{\text{diag}}^{-1}\mathcal{C}$  and  $\mathcal{P}_{\text{tri}}^{-1}\mathcal{C}$  defined in (21) and (38). We can do this using existing results from saddle point theory. For the block diagonal preconditioned problem, we use [23, Theorem 3.2, Corollary 3.3 and Corollary 3.4]. These results imply that the eigenvalues of  $\mathcal{P}_{\text{diag}}^{-1}\mathcal{C}$  depend on the eigenvalues of – in our notation –  $\tilde{\mathcal{A}}_{\text{mg}}^{-1}\mathcal{A}$  and  $\tilde{\mathcal{S}}_p^{-1}\mathcal{B}\tilde{\mathcal{A}}_{\text{mg}}^{-1}\mathcal{B}^T$ . However, in order to apply these results, both preconditioned sub-matrices must be positive definite.

To derive estimates on the eigenvalues of the block triangular preconditioned matrix, we want to apply [32, Theorem 4.1]. This result bounds the eigenvalues of  $\mathcal{P}_{\text{tri}}^{-1}\mathcal{C}$  by the eigenvalues of the preconditioned SGFE Laplacian and the preconditioned SGFE Schur complement. In our setting, it can be applied if

$$a \tilde{\mathcal{A}}_{\text{mg}} < \mathcal{A} \leq \alpha_2 \tilde{\mathcal{A}}_{\text{mg}}, \quad (41)$$

$$\hat{\gamma} \tilde{\mathcal{S}}_p \leq \mathcal{B}\mathcal{A}^{-1}\mathcal{B}^T \leq \hat{\Gamma} \tilde{\mathcal{S}}_p, \quad (42)$$

where  $a$  is the scaling introduced in (38) and  $\alpha_2$ ,  $\hat{\gamma}$  and  $\hat{\Gamma}$  are positive constants.

### 6.1 The Block Diagonal Preconditioned SGFE System

First of all, we consider the preconditioned SGFE Laplacian. To derive bounds on the eigenvalues of  $\tilde{\mathcal{A}}_{\text{mg}}^{-1}\mathcal{A}$ , we proceed as in [19, Lemma 7.2], [24, Theorem 4.6].

**Lemma 1.** *Let the matrices  $\mathcal{A}$  and  $\tilde{\mathcal{A}}_{\text{mg}}$  be defined according to (22) and (39), respectively. Then,*

$$\hat{\delta} \leq \frac{\mathbf{v}^T \mathcal{A} \mathbf{v}}{\mathbf{v}^T \tilde{\mathcal{A}}_{\text{mg}} \mathbf{v}} \leq \hat{\Delta}, \quad \forall \mathbf{v} \in \mathbb{R}^{Q_{N_u}} \setminus \{\mathbf{0}\}, \quad (43)$$

with

$$\hat{\delta} := \underline{\delta} > 0, \quad (44)$$

$$\hat{\Delta} := (\bar{\nu}_0 + \nu_\sigma)\Delta, \quad (45)$$

where  $\underline{\delta}$  is a positive constant not further specified and  $\nu_\sigma := \sum_{q=1}^{Q_z-1} g_q \bar{\nu}_q$ .

*Proof.* First of all, we bound the eigenvalues from above:

$$\lambda_{\max}(\tilde{\mathcal{A}}_{\text{mg}}^{-1} \mathcal{A}) = \max_{\mathbf{v} \in \mathbb{R}^{Q_z N_u} \setminus \{\mathbf{0}\}} \frac{\mathbf{v}^T \left( I \otimes A_0 + \sum_{q=1}^{Q_z-1} G_q \otimes A_q \right) \mathbf{v}}{\mathbf{v}^T \left( I \otimes \tilde{\mathcal{A}}_{\text{mg}} \right) \mathbf{v}} \quad (46)$$

$$\begin{aligned} &\leq \lambda_{\max} \left( I \otimes \tilde{\mathcal{A}}_{\text{mg}}^{-1} A_0 \right) + \sum_{q=1}^{Q_z-1} \lambda_{\max} \left( G_q \otimes \tilde{\mathcal{A}}_{\text{mg}}^{-1} A_q \right) \\ &\stackrel{(31),(36)}{\leq} \bar{\nu}_0 \Delta + \sum_{q=1}^{Q_z-1} g_q \bar{\nu}_q \Delta = (\bar{\nu}_0 + \nu_\sigma) \Delta. \end{aligned} \quad (47)$$

An analog procedure for the lower bound on the eigenvalues yields

$$\lambda_{\min}(\tilde{\mathcal{A}}_{\text{mg}}^{-1} \mathcal{A}) \geq \underline{\nu}_0 \delta - \nu_\sigma \Delta. \quad (48)$$

However, due to the rough bounds  $g_q$  entering  $\nu_\sigma$ , expression (48) is likely to be negative. This does not contradict the theory, but the results for the block diagonal preconditioned saddle point problem do not hold for a negative lower bound. The discrete well-posedness assumption ensures the existence of a positive lower bound  $\lambda_{\min}(\mathcal{A}) \geq \underline{\alpha} > 0$  as it implies discrete coercivity. As  $\tilde{\mathcal{A}}_{\text{mg}}^{-1}$  is positive definite as well, there is also a positive constant  $\underline{\delta}$  fulfilling

$$\lambda_{\min}(\tilde{\mathcal{A}}_{\text{mg}}^{-1} \mathcal{A}) \geq \underline{\delta} > 0, \quad (49)$$

such that the result can be applied. However, we do not have any further information on  $\underline{\delta}$ , especially not on the parameter dependencies hidden in the bound.  $\blacksquare$

Bounds on the eigenvalues of  $\tilde{\mathcal{S}}_p^{-1} \mathcal{B} \tilde{\mathcal{A}}_{\text{mg}}^{-1} \mathcal{B}^T$  can be derived as in [19, Lemma 7.3]:

**Lemma 2.** [19, Lemma 7.3] *Let  $\tilde{\mathcal{A}}_{\text{mg}}$  and  $\tilde{\mathcal{S}}_p$  be defined as in (39) and (40). Then*

$$\delta \theta \gamma^2 \leq \frac{\mathbf{q}^T \mathcal{B} \tilde{\mathcal{A}}_{\text{mg}}^{-1} \mathcal{B}^T \mathbf{q}}{\mathbf{q}^T \tilde{\mathcal{S}}_p \mathbf{q}} \leq \Delta \Theta, \quad \forall \mathbf{q} \in \mathbb{R}^{Q_z N_p} \setminus \{\mathbf{0}, \mathbf{1}\}, \quad (50)$$

*Proof.* See proof of [19, Lemma 7.3].  $\blacksquare$

The constants in the bounds in (50) only depend on the degree and type of finite elements we use and on the shape of the considered domain. They do not depend on discretization or modeling parameters.

Combining Lemma 1 and Lemma 2 with the results [23, Theorem 3.2, Corollary 3.3 and Corollary 3.4], we find that the eigenvalues of  $\mathcal{P}_{\text{diag}}^{-1}\mathcal{C}$  are bounded by a combination of (44), (45) and the bounds in (50). The bounds in (50) are parameter independent, so we look into (44) and (45). The bound (45) suggests that the eigenvalues change with the functions  $\nu_q$ ,  $q = 0, \dots, Q_z - 1$  and the parameters contained in the SG matrix bound  $g_q$ . Looking at the definition (36), the eigenvalues might thus be influenced by the chaos degree  $k$  and the KLE truncation index  $M$ . Lastly, we consider (44): As we do not have information on the parameter dependencies hidden in  $\underline{\delta}$ , any other problem parameter – such as the mesh width  $h$  – can potentially influence the eigenvalues.

## 6.2 The Block Triangular Preconditioned SGFE System

In order to bound the eigenvalues of  $\mathcal{P}_{\text{tri}}^{-1}\mathcal{C}$  using [32, Theorem 4.1], we need to fulfill (41) and (42). The right bound of (43) is an upper bound fulfilling (41) but the left bound of (43) is not necessarily a lower bound fulfilling (41). The lower bound in (41) is in fact the stronger condition:

$$\frac{\mathbf{v}^T \mathcal{A} \mathbf{v}}{\mathbf{v}^T a \tilde{\mathcal{A}}_{\text{mg}} \mathbf{v}} > 1, \quad \forall \mathbf{v} \in \mathbb{R}^{Q N_u} \setminus \{\mathbf{0}\}. \quad (51)$$

or equivalently

$$\lambda_{\min} \left( (a \tilde{\mathcal{A}}_{\text{mg}})^{-1} \mathcal{A} \right) = \min_{\mathbf{v} \in \mathbb{R}^{Q N_u} \setminus \{\mathbf{0}\}} \frac{\mathbf{v}^T \mathcal{A} \mathbf{v}}{\mathbf{v}^T a \tilde{\mathcal{A}}_{\text{mg}} \mathbf{v}} > 1. \quad (52)$$

Now, the scalar  $a$  comes into play. If it is chosen such that  $a = \kappa \lambda_{\min}(\tilde{\mathcal{A}}_{\text{mg}}^{-1} \mathcal{A})$  with  $0 < \kappa < 1$ , then a scaled preconditioner  $\kappa \lambda_{\min}(\tilde{\mathcal{A}}_{\text{mg}}^{-1} \mathcal{A}) \tilde{\mathcal{A}}_{\text{mg}}$  fulfills (52) with

$$\lambda_{\min} \left( (\kappa \lambda_{\min}(\tilde{\mathcal{A}}_{\text{mg}}^{-1} \mathcal{A}) \tilde{\mathcal{A}}_{\text{mg}})^{-1} \mathcal{A} \right) = \kappa^{-1} > 1. \quad (53)$$

However, as we have no quantitative access to the analytical lower bound (44), we need to estimate the minimum eigenvalue of  $\tilde{\mathcal{A}}_{\text{mg}}^{-1} \mathcal{A}$  numerically. A scaled preconditioner with a numerically computed positive  $a = a^* < \lambda_{\min}(\tilde{\mathcal{A}}_{\text{mg}}^{-1} \mathcal{A})$  then yields a modified version of (43), namely

$$1 < \frac{\hat{\delta}}{a^*} \leq \frac{\mathbf{v}^T \mathcal{A} \mathbf{v}}{\mathbf{v}^T a^* \tilde{\mathcal{A}}_{\text{mg}} \mathbf{v}} \leq \frac{\hat{\Delta}}{a^*}, \quad \forall \mathbf{v} \in \mathbb{R}^{Q N_u} \setminus \{\mathbf{0}\}, \quad (54)$$

which fulfills (41).

As we have assumed well-posedness of the discrete SGFE problem, a discrete inf-sup condition is fulfilled [17, Theorem 3.18]. Using the discrete representations of the norms and inner products in the FE and SG basis, we can rearrange

the discrete inf-sup condition to derive a relation exactly as in [17, Lemma 3.48 and section 3.6.6]. In our SGFE setting, the spectral equivalence has the form

$$\beta^2 \leq \frac{\mathbf{q}^T (I \otimes BA^{-1}B^T) \mathbf{q}}{\mathbf{q}^T (I \otimes M_p) \mathbf{q}} \leq 1, \quad \forall \mathbf{q} \in \mathbb{R}^{Q_{N_p}} \setminus \{\mathbf{0}, \mathbf{1}\}. \quad (55)$$

Here,  $\beta$  is the inf-sup constant of the mixed SGFE problem. We use (55) to derive bounds for the preconditioned SGFE Schur complement in the following lemma.

**Lemma 3.** *Let the Schur complement be defined by  $\mathcal{S} = -\mathcal{B}\mathcal{A}^{-1}\mathcal{B}^T$  with building blocks  $\mathcal{A}$  and  $\mathcal{B}$  in (22) and (23), and  $\tilde{\mathcal{S}}_p = I \otimes D_p$  according to (40). Then,*

$$\hat{\gamma} \leq \frac{\mathbf{q}^T \mathcal{B}\mathcal{A}^{-1}\mathcal{B}^T \mathbf{q}}{\mathbf{q}^T (I \otimes D_p) \mathbf{q}} \leq \hat{\Gamma}, \quad \mathbf{q} \in \mathbb{R}^{Q_{N_p}} \setminus \{\mathbf{0}, \mathbf{1}\}, \quad (56)$$

with

$$\hat{\gamma} := (\underline{\nu}_0 + \nu_\sigma)^{-1} \theta \beta^2, \quad (57)$$

$$\hat{\Gamma} := \underline{\delta}^{-1} \Delta \Theta. \quad (58)$$

*Proof.* We want to modify (55) in order to derive (56). The denominators are matched directly via (33) as the additional identity matrices do not change the bounds. The connection between the nominators is not that obvious. We start by considering

$$(I \otimes A)^{-1} \mathcal{A} = I \otimes A^{-1} A_0 + \sum_{q=1}^{Q_\nu-1} G_q \otimes A^{-1} A_q. \quad (59)$$

Extracting the weighting factors from the FE Laplacians yields

$$-\bar{\nu}_q \leq \frac{\mathbf{v}^T A_q \mathbf{v}}{\mathbf{v}^T A \mathbf{v}} \leq \bar{\nu}_q, \quad (60)$$

for all  $q = 1, \dots, Q_\nu - 1$  and for all  $\mathbf{v} \in \mathbb{R}^{N_u} \setminus \{\mathbf{0}\}$ . By combining (60) with the representation (59) and (36), we get

$$\frac{\mathbf{v}^T (I \otimes A)^{-1} \mathbf{v}}{\mathbf{v}^T \mathcal{A}^{-1} \mathbf{v}} \leq \bar{\nu}_0 + \sum_{q=1}^{Q_\nu-1} g_q \bar{\nu}_q = \bar{\nu}_0 + \nu_\sigma, \quad (61)$$

for all  $\mathbf{v} \in \mathbb{R}^{Q_{N_u}} \setminus \{\mathbf{0}\}$ . For the lower bound, we start with (43):

$$\frac{\mathbf{v}^T \mathcal{A} \mathbf{v}}{\mathbf{v}^T \tilde{\mathcal{A}}_{\text{mg}} \mathbf{v}} \geq \underline{\delta}, \quad \forall \mathbf{v} \in \mathbb{R}^{Q_{N_u}} \setminus \{\mathbf{0}\}. \quad (62)$$

As  $\tilde{\mathcal{A}}_{\text{mg}} = I \otimes \tilde{A}_{\text{mg}}$ , we can use the inverse of (30) with (62) and derive

$$\frac{\mathbf{v}^T (I \otimes A)^{-1} \mathbf{v}}{\mathbf{v}^T \mathcal{A}^{-1} \mathbf{v}} \geq \underline{\delta} \Delta^{-1}, \quad \forall \mathbf{v} \in \mathbb{R}^{Q_{N_u}} \setminus \{\mathbf{0}\}. \quad (63)$$

Now, we use the relation  $\mathbf{v} = \mathcal{B}^T \mathbf{q}$  in (61) and (62) to establish:

$$(\underline{\nu}_0 + \nu_\sigma)^{-1} \leq \frac{\mathbf{q}^T \mathcal{B} \mathcal{A}^{-1} \mathcal{B}^T \mathbf{q}}{\mathbf{q}^T \mathcal{B} (I \otimes A)^{-1} \mathcal{B}^T \mathbf{q}} \leq \underline{\delta}^{-1} \Delta, \quad (64)$$

for all  $\mathbf{q} \in \mathbb{R}^{Q_{N_p}} \setminus \{\mathbf{0}, \mathbf{1}\}$ . Multiplying the positive expressions (55) and (64) and using (33) then yields the assertion. ■

Using (54) and Lemma 3 with the result [32, Theorem 4.1] implies, that the eigenvalues of  $\mathcal{P}_{\text{tri}}^{-1} \mathcal{C}$  with  $a = a^* < \lambda_{\min}(\tilde{\mathcal{A}}_{\text{mg}}^{-1} \mathcal{A})$  can be bounded by a combination of the bounds in (54), (57) and (58). The upper bound in (54) and (57) suggest that the eigenvalues are influenced by the scaling  $a^*$ , the chaos degree  $k$  and the KLE truncation index  $M$  hidden in the bounds  $g_q$ , and the functions  $\nu_q$ . However, we do not know which parameters are hidden in (44) and (58). Therefore, we can not exclude the possibility that the eigenvalues change with other problem parameters such as the mesh width  $h$ .

We now introduce the matrix

$$\mathcal{H} := \begin{bmatrix} \mathcal{A} - a \tilde{\mathcal{A}}_{\text{mg}} & 0 \\ 0 & \tilde{\mathcal{S}}_p \end{bmatrix}, \quad (65)$$

with  $a = \kappa \lambda_{\min}(\tilde{\mathcal{A}}_{\text{mg}}^{-1} \mathcal{A})$ ,  $0 < \kappa < 1$ ,  $\tilde{\mathcal{A}}_{\text{mg}}$  and  $\tilde{\mathcal{S}}_p$  according to (39) and (40). We need this matrix in the following lemma, which can be proven because of the modifications to the block triangular preconditioner  $\mathcal{P}_{\text{tri}}$  in (38).

**Lemma 4.** *Let  $a$  in (38) be set to  $a = \kappa \lambda_{\min}(\tilde{\mathcal{A}}_{\text{mg}}^{-1} \mathcal{A})$ , with  $0 < \kappa < 1$ . Then, the matrix  $\mathcal{H}$  in (65) defines an inner product and the triangular preconditioned system matrix  $\mathcal{P}_{\text{tri}}^{-1} \mathcal{C}$  with  $\mathcal{C}$  and  $\mathcal{P}_{\text{tri}}$  according to (21) and (38), is  $\mathcal{H}$ -symmetric and  $\mathcal{H}$ -positive definite, i.e.*

$$\mathcal{H} \mathcal{P}_{\text{tri}}^{-1} \mathcal{C} = (\mathcal{P}_{\text{tri}}^{-1} \mathcal{C})^T \mathcal{H}, \quad (66)$$

$$\mathbf{z}^T \mathcal{H} \mathcal{P}_{\text{tri}}^{-1} \mathcal{C} \mathbf{z} > 0, \quad \forall \mathbf{z} \in \mathbb{R}^{Q_N} \setminus \{\mathbf{0}\}. \quad (67)$$

*Proof.* See proof of [19, Lemma 8.1]. ■

Bramble and Pasciak discovered the extraordinary effect of the matrix  $\mathcal{H}$  in their 1988 paper [7]. They considered a triangular preconditioned problem structurally equivalent to  $\mathcal{P}_{\text{tri}}^{-1} \mathcal{C}$ . Due to the conditions verified in Lemma 4, a conjugate gradient method exists in the  $\mathcal{H} \mathcal{P}_{\text{tri}}^{-1} \mathcal{C}$ -inner product [12]. The Bramble-Pasciak conjugate gradient (BPCG) method introduced in [7] can thus also be applied to the SGFE problem considered in this work.

## 7 Iterative Solvers

In the following, we discuss two different iterative solvers for our SGFE Stokes problem. Similar investigations were conducted in [21] for Stokes flow with deterministic data and in [19] for Stokes flow with uniform random data.



As the system matrix  $\mathcal{C}$  of the SGFE Stokes problem (20) is symmetric but indefinite (see (26)), the MINRES method is the first iterative solver one usually considers. It is attractive from a complexity point of view as the Krylov basis is built with short recurrence. However, MINRES relies on the symmetry of the problem and can thus only be combined with a symmetric preconditioner. Applying e.g. the nonsymmetric  $\mathcal{P}_{\text{tri}}$  in (38) may prevent MINRES from converging. Concerning the preliminary considerations in the sections 5 and 6, we will thus use MINRES solely in combination with  $\mathcal{P}_{\text{diag}}$  in (38). The MINRES algorithm can be formulated efficiently such that the only matrix-vector operations necessary per iteration are the application of  $\mathcal{C}$  and  $\mathcal{P}_{\text{diag}}^{-1}$ , see [8, Algorithm 4.1]. Bounds on the extreme eigenvalues of  $\mathcal{P}_{\text{diag}}^{-1}\mathcal{C}$  are often used to assess MINRES convergence behavior a priori. This is done because of the standard convergence result [8, Theorem 4.14] which bounds MINRES iteration counts by a function of those eigenvalues. Following this reasoning, we will use the results from subsection 6.1 to interpret the numerical MINRES results in section 8.

The SGFE problem is no longer symmetric when  $\mathcal{P}_{\text{tri}}^{-1}$  in (38) is applied to  $\mathcal{C}$ . Faber and Manteuffel [12] proved that there does not exist a short recurrence for generating an orthogonal Krylov subspace basis for every nonsymmetric matrix. However, they showed that there are special cases for which it is possible. The combination of  $\mathcal{P}_{\text{tri}}^{-1}\mathcal{C}$  and  $\mathcal{H}$  is such a case, as condition (66) holds. Systems of equations associated with the nonsymmetric matrix  $\mathcal{P}_{\text{tri}}^{-1}\mathcal{C}$  can thus be solved with a CG method. Besides this big advantage, there are also drawbacks: firstly, for the method to be defined properly, we must scale  $\tilde{\mathcal{A}}_{\text{mg}}$  such that (52) holds. This can be achieved by choosing the scaling as  $a = \kappa \lambda_{\min}(\tilde{\mathcal{A}}_{\text{mg}}^{-1}\mathcal{A})$ ,  $0 < \kappa < 1$ , as discussed in section 6.2. However, solving the associated eigenproblem numerically leads to additional computational costs. Secondly, the naive BPCG algorithm is associated with the  $\mathcal{H}\mathcal{P}_{\text{tri}}^{-1}\mathcal{C}$ -inner product [1, section 4]. Evaluating quantities in this inner product would lead to additional matrix-vector operations. Due to certain properties of CG methods [1], these additional costs can be avoided by reformulating the algorithm. Thereby, a BPCG algorithm can be found which needs only one extra operation compared to preconditioned MINRES [21, section 3.1]: a matrix-vector multiplication with  $\mathcal{B}$ . This additional operation originates from the definition of  $\mathcal{P}_{\text{tri}}$  in (38) and is cheap compared to a multiplication with  $\mathcal{A}$ , because  $\mathcal{B}$  is block diagonal with sparse blocks. For this reason, the BPCG method is particularly interesting in our setting where  $\mathcal{A}$  is block dense [10, Lemma 28]. There is also a convergence result for CG which bounds its iteration counts by a function of the extreme eigenvalues of  $\mathcal{P}_{\text{tri}}^{-1}\mathcal{C}$  [15, Theorem 9.4.12], so we follow the same arguments as above: We use the results from subsection 6.2 to interpret the numerical CG results in section 8.

## 8 Numerical Experiments

In the following, we compare the solvers discussed in section 7 numerically. We use the regularized driven cavity test case and investigate the performance of the two methods as well as their convergence behavior.

We associate the random field  $\mu(x, \omega)$  with the separable exponential covariance function  $C_\mu : D \times D \rightarrow \mathbb{R}$ :

$$C_\mu(x, y) = \sigma_\mu^2 e^{-|x_1 - y_1|/b_1 - |x_2 - y_2|/b_2}, \quad (68)$$

with correlation lengths  $b_1$  and  $b_2$  in the  $x_1$  and  $x_2$  direction, respectively. Eigenpairs of the two-dimensional integral operator associated with (68) are constructed by combining the eigenpairs of two one-dimensional operators, which can be calculated analytically [13, section 5.3], [18, section 7.1].

We use a regularized version of the lid-driven cavity [8, section 3.1] as our test case. The spatial domain is the unit square  $D = [-0.5, 0.5] \times [-0.5, 0.5]$  and we impose a parabolic flow profile  $u(x) = (1 - 16x_1^4, 0)^T$  at the top lid. No-slip conditions are enforced everywhere else on the boundary. For the numerical simulations, we use the following default parameter set:

$$h = 0.01, \quad k = 1, \quad M = 10, \quad \nu_0 = 1, \quad \sigma_\nu = 0.2, \quad b_1 = b_2 = 1. \quad (69)$$

If not specified otherwise, the simulation parameters are the ones in (69). The mean and variance of the corresponding velocity streamline field can be found in Figure 1.

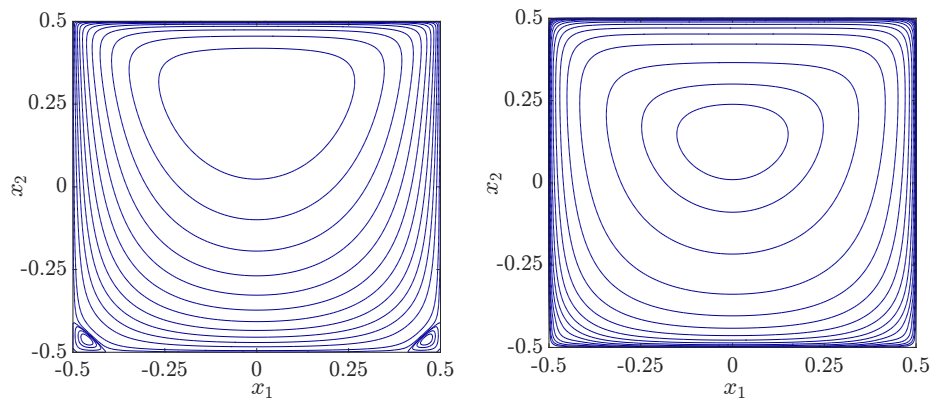


**Fig. 1.** Contour lines of the mean (left) and variance (right) of the stream function of the regularized driven cavity test case computed with the parameters in (69).

All numerical simulations are carried out in our own finite element implementation in MATLAB [28], except the setup of the multigrid preconditioner. For this particular issue, we resort to the algebraic multigrid implementation in the IFISS package [9] with two point Gauss-Seidel pre- and post-smoothing sweeps. In order to compare  $\mathcal{P}_{\text{diag}}$ -preconditioned MINRES ( $\mathcal{P}_{\text{diag}}$ -MINRES) and  $\mathcal{P}_{\text{tri}}$ -preconditioned BPCG ( $\mathcal{P}_{\text{tri}}$ -BPCG), we look at the iteration counts necessary to reduce the Euclidean norm of the relative residual below  $10^{-6}$ . As the initial

guess is always the zero vector, we thus consider numbers  $n$  such that

$$\|\mathbf{r}^{(n)}\| = \|\mathbf{b} - \mathcal{C}\mathbf{z}^{(n)}\| \leq 10^{-6}\|\mathbf{b}\|. \quad (70)$$

Before we commence with the actual comparison, we want to assess the influence of the scaling factor  $a$  on the  $\mathcal{P}_{\text{tri}}$ -BPCG convergence. Based on the reference value  $a^* \approx \lambda_{\min}(\tilde{\mathcal{A}}_{\text{mg}}^{-1}\mathcal{A})$  that we compute with MATLAB's (version 8.6.0) numerical eigensolver `eigs`, we solve the driven cavity problem for different values of the relative scaling  $a/a^*$ . Corresponding iteration counts for  $\mathcal{P}_{\text{tri}}$ -BPCG are displayed in Table 1. The minimum iteration count of 32 is attained when the scaling  $a$  is chosen to be the reference value  $a^*$ . Consequently, the ideal scaling of the preconditioner is close to the border of the  $\mathcal{H}$ -positive definiteness condition (52). However, we notice that moderate variations around the optimal scaling do not lead to a significant increase in iteration counts. Further, we can not guarantee convergence for the algorithm when  $a/a^* > 1$  as the  $\mathcal{H}$ -positive definiteness requirement (52) is no longer strictly fulfilled. Still, we could not observe divergent behavior in our experiments.

To lower the costs associated with computing  $a^*$ , we solve the associated eigenproblems on the coarsest mesh with  $h = 0.1$ . This is somewhat heuristic as we could not show  $h$ -independence of the bounds in Lemma 1. Nevertheless, we assume that the mesh size does not influence the scaling significantly due to the chosen spectrally equivalent FE preconditioners, see subsection 5.1.

**Table 1.**  $\mathcal{P}_{\text{tri}}$ -BPCG iteration counts for different values of the relative scaling  $a/a^*$ .

$a/a^*$	0.1	0.4	0.6	0.8	0.9	1.0	1.1	1.2	1.4	1.6	2.0	3.0	5.0
$n$	46	41	39	35	34	32	35	35	35	36	38	41	42

We now look at the iteration counts of the two solvers when different parameters are varied, starting with the mesh size  $h$  and the truncation index  $M$  of the KLE. The associated numerical results are displayed in Figure 2. First of all, we observe that  $\mathcal{P}_{\text{tri}}$ -BPCG converges in fewer iterations than  $\mathcal{P}_{\text{diag}}$ -MINRES for all considered values of  $h$  and  $M$ . Further, the iteration counts of both solvers do not increase under mesh refinement but rather decrease slightly, as can be seen in the left plot. In the right plot, we notice that the iteration counts increase up to  $M \approx 5$  for both methods and then basically stay constant independent of  $M$ . The results in Figure 2 suggest that the iteration counts are asymptotically independent of the mesh size and the KLE truncation index. This is according to expectations for  $h$ , as the multigrid V-cycle and the diagonal of the pressure mass matrix are spectrally equivalent to the weighted FE Laplacians and Schur complement, see (30) – (34). Asymptotic independence of  $M$  is somewhat surprising, as this parameter appears in (45), hidden in  $\nu_\sigma$ . This dependence originates from the bounds on the SG matrices in (36).

Figure 3 visualizes the convergence behavior of the two considered solvers when either the total degree  $k$  of the chaos basis or the standard deviation  $\sigma_\mu$

of the original Gaussian process  $\mu(x, \omega)$  in (2) is varied. We again observe that  $\mathcal{P}_{\text{diag-MINRES}}$  consistently needs more iterations to converge than  $\mathcal{P}_{\text{tri-BPCG}}$ . We can further see a steady increase of iteration counts with both  $k$  and  $\sigma_\mu$  for both solvers. That was to be expected as these parameters also occur in the bounds (45) and (57). When they increase, the fluctuation parts – i.e. the terms in the sum in (22) – become more important, see (17) and (36).

In order to alleviate the influence on  $k$  and  $\sigma_\mu$ , one needs to use more advanced approaches for the SG preconditioners such as the Kronecker product preconditioner, see [24,27]. However, as there is – to the best of our knowledge – no practical preconditioner that can eliminate just one of these dependencies and using a more elaborate preconditioner also results in increased computational costs, we do not investigate this issue further here.

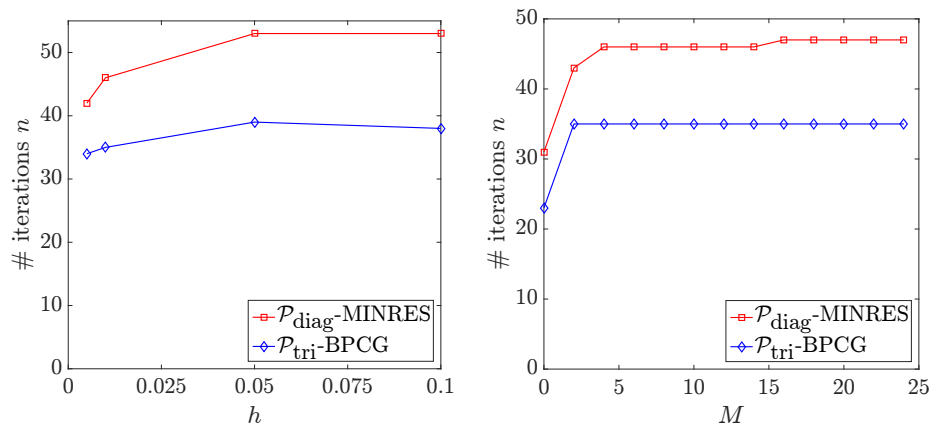


**Fig. 2.** Iteration counts for different values of the mesh size  $h$  (left) and the KLE truncation index  $M$  (right) for  $\mathcal{P}_{\text{diag-MINRES}}$  (red) and  $\mathcal{P}_{\text{tri-BPCG}}$  (blue).

## 9 Conclusion

The construction of our BPCG solver relies on the appropriate choice of the scaling  $a$  such that the matrix  $\mathcal{H}$  is positive definite. Choosing  $a$  close to the minimum eigenvalue of the preconditioned SGFE Laplacian is optimal, as confirmed by the numerical experiments. However, solving the associated eigenproblem numerically is often prohibitive. To reduce the costs of computing  $a$ , one can solve the eigenproblem on a coarser mesh. This approach worked well in the numerical examples we considered.

We compared the iteration counts of two iterative solvers with structurally different preconditioners: block diagonal preconditioned MINRES and block triangular preconditioned BPCG. The iteration counts of the latter were consistently lower in our experiments. However, as we used the same FE and SG

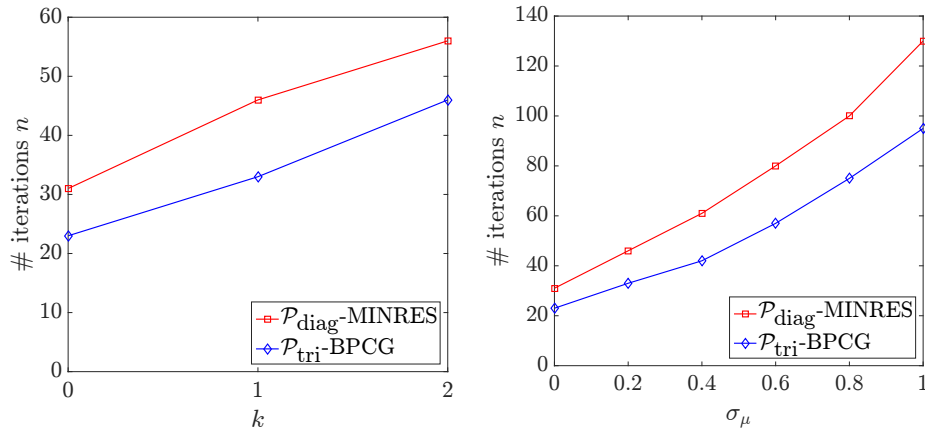


**Fig. 3.** Iteration counts for different values of the chaos degree  $k$  (left) and the standard deviation  $\sigma_\nu$  (right) of the Gaussian field  $\mu(x, \omega)$  for  $\mathcal{P}_{\text{diag}}\text{-MINRES}$  (red) and  $\mathcal{P}_{\text{tri}}\text{-BPCG}$  (blue).

building blocks, the performance was qualitatively the same: The application of the multigrid preconditioner and the diagonal of the pressure mass matrix resulted in iteration counts basically independent of the mesh width  $h$ . The input dimension  $M$  is a measure for the accuracy of the input representation. However, as soon as a certain threshold is reached, the iteration counts stayed constant independent of  $M$ . This suggests that the eigenvalues of the SG matrices are asymptotically independent of  $M$ , an assertion which is not according to the current theory. Both the degree of the polynomial chaos  $k$  as well as the standard deviation  $\sigma_\mu$  critically influence the condition of our preconditioned problems. This is already visible in the available eigenvalue bounds. The mean-based SG preconditioner can not alleviate these influences. Therefore, when we increased one of these parameters, iteration counts increased as well.

Summarizing the investigations of the BPCG method with block triangular preconditioner and the MINRES method with block diagonal preconditioner, we can state the following: The eigenvalue analysis is largely inconclusive mainly due to the coarse inclusion bounds for the eigenvalues of the SG matrices. However, our numerical tests suggest that the methods perform similarly to each other and essential behave as expected. If the scaling parameter can be obtained cheaply, the application of the block triangular preconditioner can result in a noticeable reduction of iteration counts compared to the application of the block diagonal preconditioner. This can lead to a reduction of the overall computational costs, because one step of block diagonal preconditioned MINRES is – especially in the SGFE case – only marginally cheaper than one step of block triangular preconditioned BPCG.

**Acknowledgment.** This work is supported by the Excellence Initiative of the

German federal and state governments and the Graduate School of Computational Engineering at Technische Universität Darmstadt.

## References

1. Ashby, S. F., Manteuffel, T. A., Saylor, P. E.: A taxonomy for conjugate gradient methods, *SIAM J. Numer. Anal.* 27(6), pp. 1542–1568 (1990). doi:10.1137/0727091
2. Babuška, I., Tempone, R., Zouraris G. E.: Galerkin finite element approximations of stochastic elliptic partial differential equations, *SIAM J. Numer. Anal.* 42(2), pp. 800–825 (2004). doi:10.1137/S0036142902418680
3. Babuška, I., Nobile, F., Tempone, R.: A stochastic collocation method for elliptic partial differential equations with random input data, *SIAM J. Numer. Anal.* 45(3), pp. 1005–1034 (2007). doi:10.1137/050645142
4. Bachmayr, M., Cohen, A., DeVore, R., Migliorati, G.: Sparse polynomial approximation of parametric elliptic PDEs. Part II: lognormal coefficients, *ESAIM: M2AN* 51(1), pp. 341–363 (2017), 10.1051/m2an/2016051
5. Benzi, M., Golub, G. H., Liesen, J.: Numerical solution of saddle point problems. *Acta Numerica* 14, pp. 1–137 (2005). doi:10.1017/S0962492904000212
6. Bespalov, A., Powell, C. E., Silvester, D.: A priori error analysis of stochastic Galerkin mixed approximations of elliptic PDEs with random data, *SIAM J. Numer. Anal.* 50(4), pp. 2039–2063 (2012). doi:10.1137/110854898
7. Bramble, J. H., Pasciak, J. E.: A preconditioning technique for indefinite systems resulting from mixed approximations of elliptic problems, *Mathematics of Computation* 50(181), pp. 1–17 (1988). doi:10.1090/S0025-5718-1988-0917816-8
8. Elman, H. C., Silvester, D. J., Wathen, A. J.: *Finite Elements and Fast Iterative Solvers: with Applications in Incompressible Fluid Dynamics*, Oxford University Press, Oxford, New York, 2nd ed. (2014)
9. Elman, H. C., Ramage, A., Silvester, D. J.: IFISS: a computational laboratory for investigating incompressible flow problems, *SIAM Review* 56(2), pp. 261–273(2014). doi:10.1137/120891393
10. Ernst, O. G., Ullmann, E.: Stochastic Galerkin matrices, *SIAM J. Matrix Anal. & Appl.*, 31(4), pp. 1848–1872 (2010). doi:10.1137/080742282
11. Ernst, O. G., Powell, C. E., Silvester, D. J., Ullmann, E.: Efficient solvers for a linear stochastic Galerkin mixed formulation of diffusion problems with random data, *SIAM J. Sci. Comput.*, 31(2), pp. 1424–1447 (2009). doi:10.1137/070705817
12. Faber, V., Manteuffel, T.: Necessary and sufficient conditions for the existence of a conjugate gradient method, *SIAM J. Numer. Anal.* 21(2), pp. 352–362 (1984). doi:10.1137/0721026
13. Ghanem, R. G., Spanos, P. D.: *Stochastic Finite Elements – a Spectral Approach*, Springer, New York (1991).
14. Gunzburger, M. D., Webster, C. G., Zhang, G.: Stochastic finite element methods for partial differential equations with random input data, *Acta Numerica* 23, pp. 521–650 (2014). doi:10.1017/S0962492914000075
15. Hackbusch W.: *Iterative Solution of Large Sparse Systems of Equations*, Springer, New York, 1st ed. (1994)
16. Hoang, V. H., Schwab, C.:  $N$ -term Wiener chaos approximation rates for elliptic PDEs with lognormal Gaussian random inputs. *Math. Models Methods Appl. Sci.* 24(4), pp. 797–826 (2014). doi:10.1142/S0218202513500681

17. John, V.: *Finite Element Methods for Incompressible Flow Problems*, Springer International Publishing, Cham, Switzerland (2016).
18. Lord, G. J., Powell, C. E., Shardlow, R.: *An Introduction to Computational Stochastic PDEs*, Cambridge University Press, New York (2014).
19. Müller, C., Ullmann, S., Lang, J.: A Bramble-Pasicak conjugate gradient method for discrete Stokes equations with random viscosity. Preprint, arXiv:1801.01838 (2018). <https://arxiv.org/abs/1801.01838>
20. Oksendal, B.: *Stochastic Differential Equations: An Introduction with Applications*, 5th edition, Springer, Berlin (1998).
21. Peters, J., Reichelt, V., Reusken, A.: Fast iterative solvers for discrete Stokes equations, *SIAM J. Sci. Comput.* 27 (2), pp. 646–666 (2005). doi:10.1137/040606028
22. Powell, C. E., Elman, H. C.: Block-diagonal preconditioning for spectral stochastic finite-element systems, *IMA Journal of Numerical Analysis* 29(2), pp. 350–375 (2009). doi:10.1093/imanum/drn014
23. Powell, C. E., Silvester, D.: Optimal preconditioning for Raviart–Thomas mixed formulation of second-order elliptic problems, *SIAM J. Matrix Anal. & Appl.* 25(3), pp. 718–738 (2003). doi:10.1137/S0895479802404428
24. Powell, C. E., Ullmann, E.: Preconditioning stochastic Galerkin saddle point systems. *SIAM J. Matrix Anal. & Appl.* 31(5), pp. 2813–2840 (2010). doi:10.1137/090777797
25. Schwab, C., Gittelson, C. J.: Sparse tensor discretizations of high-dimensional parametric and stochastic PDEs. *Acta Numerica* 20, pp. 291–467 (2011). doi:10.1017/S0962492911000055
26. Ullmann, E.: *Solution strategies for stochastic finite element discretizations*. PhD thesis, Bergakademie Freiberg University of Technology (2008).
27. Ullmann, E.: A Kronecker product preconditioner for stochastic Galerkin finite element discretizations, *SIAM J. Sci. Comput.* 32(2), pp. 923–946 (2010). doi:10.1137/080742853
28. Ullmann, S.: *Triangular Taylor Hood finite elements, version 1.4*. Retrieved: 06 October 2017. [www.mathworks.com/matlabcentral/fileexchange/49169](http://www.mathworks.com/matlabcentral/fileexchange/49169)
29. Ullmann, E., Elman, H. C., Ernst, O. G.: Efficient iterative solvers for stochastic Galerkin discretizations of log-transformed random diffusion problems, *SIAM J. Sci. Comput.* 34(2), pp. A659–A682 (2012). doi:10.1137/110836675
30. Wathen, A. J.: On relaxation of Jacobi iteration for consistent and generalized mass matrices. *Communications in Applied Numerical Methods* 7(2), pp. 93–102 (1991). doi:10.1002/cnm.1630070203
31. Xiu, D., Karniadakis, G. E.: The Wiener–Askey polynomial chaos for stochastic differential equations. *SIAM J. Sci. Comput.* 24(2), pp. 619–644 (2002). doi:10.1137/S1064827501387826
32. Zulehner, W.: Analysis of iterative methods for saddle point problems: a unified approach, *Mathematics of Computation* 71 (238), pp. 479–505 (2001). <http://www.jstor.org/stable/2698830>